J Mater Sci (2009) 44:6683–6692
DOI 10.1007/s10853-009-3573-x

MESOSTRUCTURED MATERIALS

Perfluoroalkylsulfonic acid-functionalized periodic mesostructured organosilica: a strongly acidic heterogeneous catalyst

David Dubé · Micha Rat · Wei Shen · François Béland · Serge Kaliaguine

Received: 14 October 2008 / Accepted: 12 May 2009 / Published online: 28 May 2009

Abstract Periodic mesostructured organosilicas (PMO) were synthesized using 1,2-bis(trimethoxysilyl)ethane (BTME) under acidic conditions using Pluronic 123 as surfactant. The PMO ethane-silicas were then grafted with 1,2,2-trifluoro-2-hydroxy-1-trifluoromethylethane sulfonic acid β-sultone yielding a new perfluoroalkylsulfonic acid PMO catalyst. Ordered hexagonal mesostructures (*P6mm*) with surface areas up to 500 m^2/g and narrow pore size distribution (around 5.1 nm) were obtained. This work thus provides an example of chemical modification for the conception of functionalized PMO acid catalysts. Liquid phase self-condensation of heptanal and acetalization of heptanal by 1-butanol were performed at 30 and 75 °C in the presence of these catalysts and results were compared with those obtained with several other heterogeneous hydrophobic acid catalysts.

Introduction

Periodic mesostructured organosilicas (PMOs) with organic groups bridged in the framework have opened a new area in development of heterogeneous catalysts [1–3]. Since the discovery of PMOs, various organosilica precursors with bridging organic groups such as methane, ethane, ethylene, benzene, thiophene, and biphenyl have been incorporated in the framework [4–9]. Recently, self-assembly of trimethylene-bridged cyclic silesquioxane precursor to yield the well-ordered trimethylene-bridged 3-ring PMO have been performed by Landskron and Ozin [10]. Che et al. [11] have proposed a new templating route for preparing hybrid mesoporous materials using anionic surfactants. Efforts have been made to create solid acid catalysts with strong Brönsted acidity, similar to zeolites, but with larger pore diameters accommodating larger substrates. Diaz et al. [12] have grafted mercaptopropyltrimethoxysilane on MCM-41 and MCM-48. A propylsulfonic acid moiety was then produced by the oxidative reaction of the thiol functional group with H_2O_2. This method was further applied to other mesostructured materials (FSM-16 [13] and SBA-15 [12, 13]). Lin and co-workers [14] reported a new co-condensation method to generate carboxylic and sulfonic acid-functionalized mesostructured silica MCM-41-type nanosphere materials while controlling the surface concentration of the organic functional groups. The method involves the utilization of disulfide-containing organosilanes, such as 3-[3′-(trimethoxysilyl)propyldisulfanyl]propionic acid and 2-[3-(trimethoxysilyl)propyldisulfanyl]ethanesulfonic acid sodium salt, to electrostatically match with the cationic template (CTAB) in a base-catalyzed reaction of TEOS. The presence of electron-withdrawing fluorine atoms in the structure significantly increases the acid strength of the terminal sulfonic acid group. Alvaro et al. [15, 16] presented the preparation of hybrid MCM-41 and SBA-15 silicas functionalized with perfluoroalkylsulfonic acid groups by a single-step reaction between the surface OHs of the mesostructured materials and 1,2,2-trifluoro-2-hydroxy-1-trifluoromethylethane sulfonic acid β-sultone (THTSAS). These heterogeneous catalysts yielded a better catalytic activity in the etherification of octanoic acid with ethanol

D. Dubé · M. Rat · W. Shen · S. Kaliaguine (✉)
Department of Chemical Engineering, Laval University, Quebec City, QC G1K 7P4, Canada
e-mail: serge.kaliaguine@gch.ulaval.ca

F. Béland
SiliCycle Inc., 114-1200 Ave. Saint-Jean-Baptiste, Quebec City, QC G2E 5E8, Canada

(C_8 acid conversion of 88% at 60 °C) than Nafion® (C_8 acid conversion of 57% under the above conditions). Moreover, the acylation of anisole was also possible, with high selectivity for 4-methoxyacetophenone. Hybrid material with maximum acid capacities of 0.5 mmol H^+/g was obtained. The same preparation procedure was used by Athens et al. [17] to synthesize mesostructured aluminosilica-grafted THTSAS. On the other hand, Macquarrie et al. [18] presented a nonoxidative direct synthesis of mesostructured silica-perfluorosulfonic acid materials with strong Brönsted acid sites. The materials were prepared using a perfluorosulfonic acid silane and TEOS using the sol–gel co-condensation route. The complete incorporation of both silanes gave a well-ordered material with a loading of 0.2 mmol S/g. The catalyst presents a high selectivity for the reaction between 2-methylfuran and acetone to give the bis-furan.

Acid functional groups can also be directly incorporated in PMOs. Acid silane precursors may be introduced in the PMO synthesis mixture and co-condensed with the silsesquioxane. All these techniques allow to create acid sites in a less polar organic environment while increasing the diffusivities of reactants and products owing to the large pore diameters of the sulfonic acid-functionalized PMOs so produced [19–24]. Kondo and co-workers [25, 26] have proposed a chemical modification technique to create a new type of PMO acid catalysts. In this procedure, ethylene sites at the surface of an ethylene-bridged PMO are converted to phenylene sulfonic acid groups in a two-step process. The procedure involves a Diels–Alder reaction with benzocyclobutene followed by sulfonation in the presence of H_2SO_4. Dubé et al. [27] have prepared a sulfonic acid-functionalized PMO (ethylene bridged) by chemical modification technique in two steps. First, the ethylene bridges were arylated with benzene using $AlCl_3$ as catalyst. This material was further treated with H_2SO_4 for the sulfonation of the phenyl moieties yielding the sulfonic acid-functionalized PMO. Several reactions have been tested with different sulfonic acid mesostructured silicas or organosilicas such as estherification of glycerol with fatty acid [12, 28], estherification of acetic acid with ethanol [24], synthesis of 2-ethoxytetrahydropyran from 3,4-dihydro2H-pyran and ethanol [29], synthesis of bisphenol A by condensation of phenol with acetone, alkylation of phenol with 2-propanol [23], etherification of 1-butanol [19], heptanal self-condensation [27], and liquid phase acetalization of heptanal by 1-butanol [30]. Among these reactions, all the water-producing ones should benefit from the increased hydrophobicity of the acid-functionalized PMOs.

Self-condensation of carbonyl compounds is an important reaction in synthesis of fine chemicals because it leads to C–C bond formation. This reaction can be catalyzed by acids or bases. Most of the studies in the literature have reported the self-condensation over solid base catalysts [22, 31, 32]. Moreover, acetalization is a reaction producing acetals and it is used as protecting groups for carbonyl compounds. Acetals are used in cosmetic, as fragrances, pharmaceuticals, and detergents. The homogeneous catalysts used industrially produces highly toxic waste [13, 33, 34].

Herein, we propose a simple method to produce a perfluoroalkylsulfonic acid-functionalized PMO with high acid capacities. The two-step synthesis involves an acid-catalyzed hydrolysis and condensation of 1,2-bis(trimethoxysilyl)ethane (BTME) using Pluronic P123 as the structure-directing agent followed by a soxhlet extraction. PMO was further functionalized by the grafting on its surface of the perfluoroalkylsulfonic acid group. The catalytic properties in the self-condensation of heptanal and acetalizations of heptanal by 1-butanol in which both reactions produce water were studied.

Experimental

Catalyst preparation

The designation of the catalysts reflects three characteristics of the material. Here, PMO stands for ethane silica, PF means perfluoroalkyl, and SO_3H indicates the sulfonic acid moiety so that PMO-PFSO_3H0.8 designates a perfluoroalkylsulfonic acid-functionalized ethane-silica having a loading of 0.8 mmol H^+/g. A schematic illustration of the synthetic pathway to the new sulfonic acid-functionalized PMO is shown in Fig. 1.

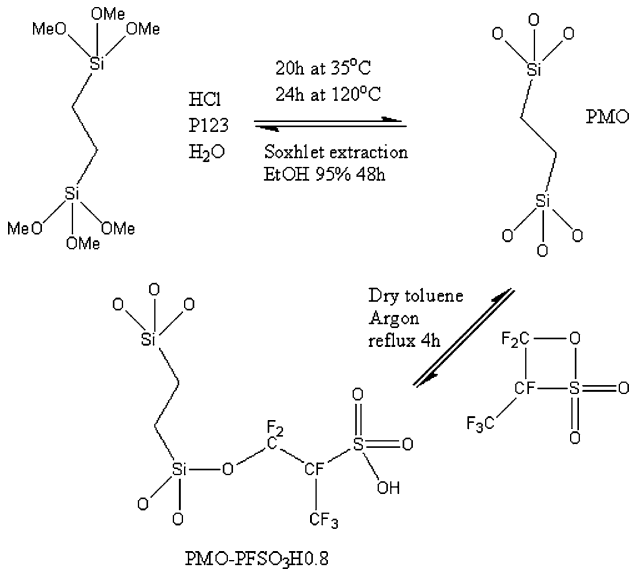

Fig. 1 Schematic representation of the two-step synthesis mechanism of PMO acid catalyst

Preparation of ethane-silica PMO

Ethane-bridged PMO samples with hexagonal symmetry were prepared using BTME and following the synthesis procedure described by Inagaki et al. [4]. In a typical synthesis, 9.64 g of Pluronic 123 (EO_{20}-PO_{70}-EO_{20}, BASF) was dissolved in 58.16 g of 2 M HCl and 250 mL of water at room temperature. After complete dissolution, the solution was heated at 40 °C before addition of 12.58 g of BTME. The resulting solution was stirred for 20 h. The synthesis gel molar composition was: 1.00:BTME; 0.039:P123; 2.84:HCl; and 414:H_2O. The resulting mixture was transferred into an autoclave for aging at 100 °C for 24 h. The gel was filtered, washed with deionized water, and dried overnight at 80 °C. The template was removed from the as-synthesized material using a Soxhlet extractor and ethanol for 48 h.

Preparation of SBA-15 mesostructured silica

SBA-15 mesostructured silica samples were prepared using tetraethyl orthosilicate (TEOS) and following the synthesis procedure described by Choi et al. [35]. In a typical synthesis, 3.46 g of P123 was dissolved in 62.8 g H_2O and 2 g of concentrated HCl (35%) at room temperature. After complete dissolution, the solution was heated at 35 °C before addition of 6.21 g of TEOS. The resulting solution was stirred for 20 h. The resulting mixture was transferred into an autoclave for aging at 100 °C for 24 h. The gel was filtered, washed with deionized water, and dried overnight at 80 °C. The template was removed from as-synthesized material by calcination at 550 °C.

Grafting procedure of THTSAS on ethane-bridged PMO and SBA-15 mesostructured silica (Schlenk technique)

The mesostructured support (2 g) was dried at 200 °C under vacuum (overnight) and kept under dry argon in a Schlenk tube. The support was added to 50 mL of toluene (sodium dried) in the reaction tube under dry argon atmosphere. To this solution was added 2 g of THTSAS (PMO-$PFSO_3H0.8$) stored at 4 °C. The mixture was refluxed for 4 h under dry argon and then filtered and washed three times with dry toluene (50 mL). The functionalized PMO and SBA-15 were dried overnight at 80 °C.

Characterization

X-ray diffraction patterns were recorded using a D4 Endeavor/Bruker AXS powder diffraction system with CuKα radiation ($\lambda = 1.5406$ Å). Diffraction patterns were recorded with scan step of 0.02° for 2θ between 0.5° and 5°.

Nitrogen adsorption/desorption isotherms were measured at liquid nitrogen temperature using a QUANTACHROME NOVA 2000 instrument. Before adsorption, the samples were evacuated at 120 °C for 6 h. Specific surface area was calculated using the BET method in the relative pressure range of 0.05–0.25. The pore diameter was estimated from the peak position of the BJH pore size distribution.

The weight loss curves (TGA) were recorded using a TA Instruments TGA model Q500 from ambient temperature to 700 °C at a heating rate of 5 °C/min under helium. The samples were dehydrated at 110 °C for 2 h before TGA analysis.

Sample compositions were established by elemental analysis using a CNS analyzer CARLO ERBA model 1500. The ion exchange capacities of the sulfonic acid catalysts were determined using aqueous solutions of NaCl (0.1 M) and NaOH (0.005 M) [20]. In a typical experiment, 0.05 g of solid was added to 10 g of NaCl solution. The resulting suspension was allowed to equilibrate and thereafter titrated by a drop wise addition of NaOH solution.

Impedance spectroscopy measurements were performed over the frequency range 1–10^7 Hz with oscillating voltage 100 mV, using a PC-controlled SI 1260 impedance/gain-phase analyzer (Solartron) at room temperature. The impedance data were corrected for contribution from the empty and short-circuited cell. The proton conduction of most solid electrolytes is a water-assisted phenomenon, which is extremely sensitive to water adsorption. The procedure for conductivity measurements used in this work is described elsewhere in detail [36].

Adsorbed pyridine infrared spectra (IR-pyridine) were recorded using a BIO-RAD FTS-60 FTIR spectrometer. The self-supporting wafers were evacuated in situ in an IR cell at 100 °C overnight. Pyridine was permitted to desorb at 25–100 °C. The spectra were recorded after cooling at room temperature.

^{29}Si MAS NMR spectra were obtained at room temperature on a BRUKER AVANCE 300 MHz. ^{29}Si NMR was recorded at a frequency of 59.6 MHz and at 4 kHz spinning rate.

Catalytic tests

Heptanal self-condensation

The liquid-phase catalytic test was performed in a glass batch reactor equipped with an in situ ATR-FTIR probe (ASI, Mettler-Toledo, USA) [19]. Linear calibration curves were established as previously described [19, 30]. Before each reaction test, the catalyst was predehydrated for 1 h under vacuum at 60 °C. This predehydration operation was found to be crucial since the contact with humid air yields

drastic catalyst deactivation [19]. Typically, 0.5 g of the dried catalyst was added to 50 mL of pure heptanal. In one series of experiments, the catalyst mass was varied from one catalyst to the next to keep the same total content of acid sites in the reactor. The reaction was carried out in absence of solvent under autogenous pressure at 30 and 75 °C. The IR spectra of the reaction medium were recorded at specific time intervals and were later processed using the React IR software. A calibration was previously realized at 30 and 75 °C with different concentrations of heptanal using the 1720 cm^{-1} band. Two hybrid mesostructured materials (ASMES: arene sulfonic acid-functionalized ethane silica [19], PMO-PSA: benzene sulfonic acid-functionalized ethylene silica [27]) and Nafion® SAC-13 were used as reference samples.

Recycle studies of the PMO-PFSO$_3$H1.3

The initial heptanal self-condensation test described above was repeated several times to study the catalyst reusability. Upon completion of a 3-h reaction test, the reaction mixture was filtered and the catalyst was washed with benzene and dried under vacuum at 60 °C. The reactor was then recharged with fresh heptanal and the used catalyst.

Acetalization of heptanal by 1-butanol

The liquid-phase catalytic test was also performed in a glass batch reactor equipped with an in situ ATR-FTIR probe (ASI, Mettler-Toledo, USA) [19]. Before each reaction test, the catalyst was predehydrated for 1 h under vacuum at 60 °C. Typically, 100 mg of dried catalyst was added to 50 mL of a mixture of 1-butanol and heptanal (molar ratio: 1-butanol/heptanal = 2). In one series of experiments, the catalyst mass was varied from one catalyst to the next to keep the same total content of acid sites in the reactor. The reaction was carried out in absence of solvent under autogenous pressure at 75 °C. The IR spectra of the reaction medium were recorded at specific time intervals and were later processed using the React IR software. A calibration of the FTIR probe was performed at the reaction temperature of 75 °C using heptanal/1-butanol mixtures of known composition. The 1720 cm^{-1} band ascribed to the elongation of the heptanal carbonyl group was used for the quantification of heptanal conversion. At the end of each test, a sample of reaction medium was injected into a GC/MS (Varian Saturn 2200) for confirmation of the reaction products and independent measurement of heptanal conversion.

Results

Characterization

Two perfluoroalkylsulfonic acid-grafted PMO catalysts were synthesized and analyzed. They were prepared using different mass ratios THTSAS/PMO (1.0 and 2.0) to obtain two different concentrations of perfluoroalkylsulfonic acid functions. The textural and compositional properties of the catalysts and their PMO supports are presented in Table 1. Nitrogen adsorption–desorption isotherms for PMOs, PMO-PFSO$_3$H0.8, and PMO-PFSO$_3$H1.3 show type IV curves according to the IUPAC nomenclature, which indicates the mesoporous nature of the catalysts. The specific surface area and pore diameter of each catalyst decrease during the OH grafting treatment. Those changes are due to the surface modification by the grafting reactions (THTSAS) onto the surface of PMOs. The sulfur content reflects the density of sulfonic acid groups, and the values

Table 1 Physicochemical properties of the catalysts and their precursors

Catalyst	Mass THTSAS/mass support	S_{BET} (m^2/g)	Pore diameter (nm)	Pore volume (mL/g)	[S] (mmol/g) (±0.01)	[H^+] (mmol/g) (±0.05)
PMO[a]	–	676	5.3	1.01	–	–
PMO[b]	–	761	5.4	1.16	–	–
SBA-15	–	697	6.5	1.05	–	–
PMO-PFSO$_3$H0.8	1.0	468	4.9	0.71	0.83	0.85
PMO-PFSO$_3$H1.3	2.0	504	5.1	0.70	1.27	1.30
SBA-PFSO$_3$H0.2	1.0	534	6.5	0.80	0.22	0.25
ASMES [15]	–	780	6.0	1.16	0.81	0.84
PMO-PSA [29]	–	725	5.5	1.08	0.83	0.87
Nafion® SAC-13	–	200[c]	10[c]	–	0.12[c]	–

[a] PMO ethane-silica used for the preparation of PMO-PFSO$_3$H0.8

[b] PMO ethane-silica used for the preparation of PMO-PFSO$_3$H1.3

[c] Values supplied by the manufacturer

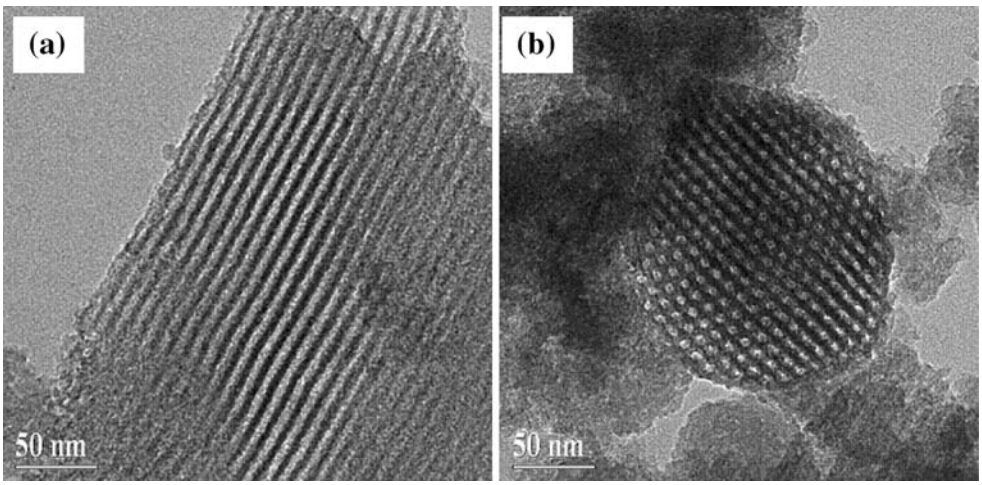

Fig. 2 TEM images of PMO-PFSO$_3$H0.8. **a** Side. **b** Top

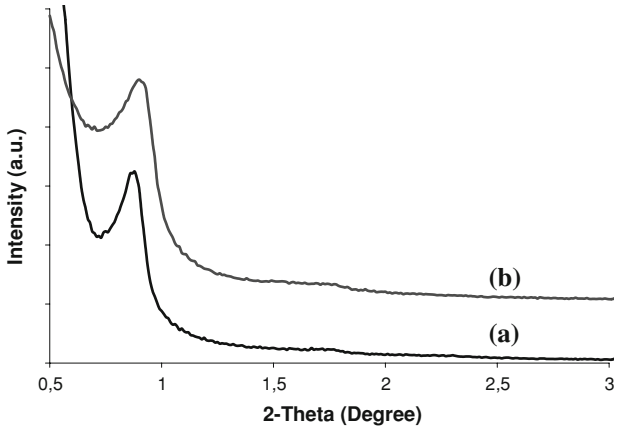

Fig. 3 X-ray diffraction pattern of (*a*) PMO and (*b*) PMO-PFSO$_3$H0.8

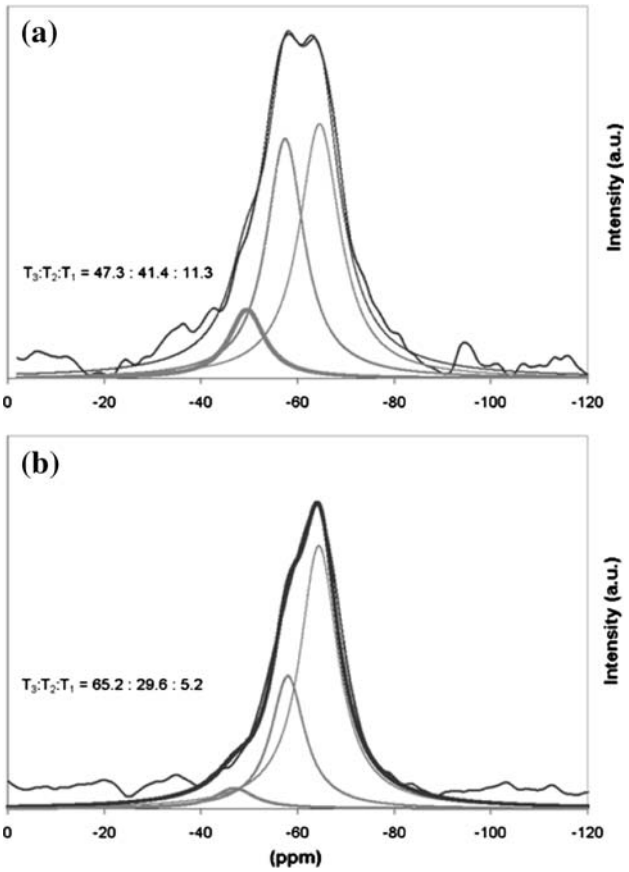

Fig. 4 ^{29}Si MAS NMR spectra of (**a**) PMO and (**b**) PMO-PFSO$_3$H0.8

reported in Table 1 indicate that the lowest mass ratio THTSAS/PMO results in a lower content of grafted sulfonic acid groups. The TEM images (Fig. 2) and XRD data (Fig. 3) show that the mesoporous structure is preserved after the chemical modification. Diffraction peaks in XRD pattern and regular hexagonal arrangement in TEM images reveal that the synthesized material has the characteristic of 2-d hexagonal (*P6mm*) structure, which indicates that the ordering of the PMO is not affected by the grafting of perfluoroalkylsulfonic acid function. Compared to the initial PMO, it is found that the 100 peak of PMO-PFSO$_3$H0.8 sample is slightly shifted toward higher diffraction angles after the grafting operation, likely associated with the average decrease in pore diameter due to the introduction of the perfluoroalkylsulfonic acid function.

Figure 4 shows the ^{29}Si MAS NMR spectra of the PMO support and the PMO-PFSO$_3$H0.8 with the deconvolution curves of each peak. The PMO presented three peaks at −64,−57, and −47 ppm attributable to T^3 [RSi(OSi)$_3$], T^2 [RSi(OSi)$_2$OH], and T^1 [RSi(OSi)(OH)$_2$] resonances, respectively [37]. For the PMO support, the surface ratios of the peak components associated to these silica species are recognized to be T^3:T^2:T^1 = 47.3:41.4:11.3. After grafting step, T^2 decreases, T^3 increases, and the ratio becomes T^3:T^2:T^1 = 65.2:29.6:5.2. These results indicate that the

perfluoroalkylsulfonic acid is grafted on the surface of the PMO as the increase in T^3 corresponds to the disappearance of some of the support OHs. There is no occurrence of Q^n $[Si(OSi)_n(OH)_{4-n}]$ resonances which attests that essentially all silicon atoms were covalently bound to carbon.

The thermogravimetric curves for the PMO-$PFSO_3H$1.3 catalyst sample are shown in Fig. 5. The differential thermogravimetric analysis for PMO-$PFSO_3H$1.3 shows three peaks. The peak centered at 180 °C corresponds to the decomposition of the sulfonic acid groups. The peak at 450 °C is ascribed to the perfluoroalkyl groups. The peak at 580 °C is due to the thermal degradation of the ethane-silica framework of the support.

The kind of acid sites of the catalysts were characterized using FTIR spectra of adsorbed pyridine (pyridine-FTIR). Spectra of the PMO-$PFSO_3H$0.8 evacuated at 50 and 75 °C show two bands (1490 and 1550 cm^{-1}) attributed to pyridine adsorbed on Brönsted acid sites (Fig. 6). The band at 1550 cm^{-1} is attributed to Brönsted acid sites, and the band at 1490 cm^{-1} may belong to both Brönsted and Lewis acid sites [38]. The absence of any line in the 1450 cm^{-1} area indicates a complete absence of Lewis acid sites. The band at 1440 cm^{-1} observed before desorption is associated with physisorbed pyridine. The nonfunctionalized PMOs did not display significant pyridine FTIR signals (not shown), indicating that these PMOs have no acidic properties. For both temperatures, the only acid species detected on the sulfonic acid-functionalized catalyst were Brönsted acid sites.

Impedance spectroscopy was used to determine the proton conductivity of the perfluoroalkylsulfonic acid-functionalized PMOs. The obtained conductivity results are presented in Fig. 7. As expected, the proton conductivity increases with water content. The maximum value obtained for PMO-$PFSO_3H$1.3 and PMO-FSO_3H0.8 at a water content around 100 and 150% is 1.0×10^{-1} and 5.8×10^{-2} S/cm, respectively (expressed as weight percent compared to the dry material). Nafion® SAC-13 presented a lower conductivity at 2.8×10^{-3} S/cm. Moreover, the comparison between acid catalysts revealed that the proton conductivity is proportional to the acid site density.

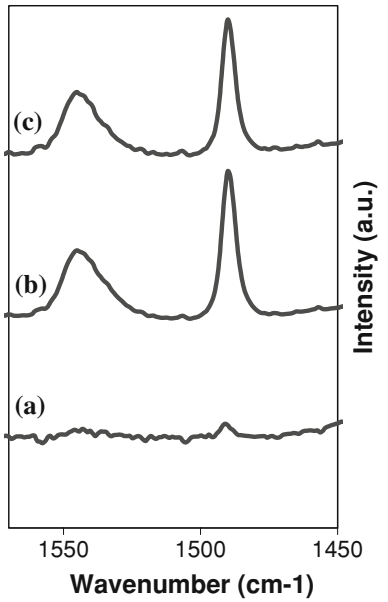

Fig. 6 FTIR spectra of PMO-$PFSO_3H$0.8 (*a*) evacuated at 100 °C before pyridine adsorption, after pyridine adsorption and evacuation (*b*) at 50 °C, and (*c*) 75 °C

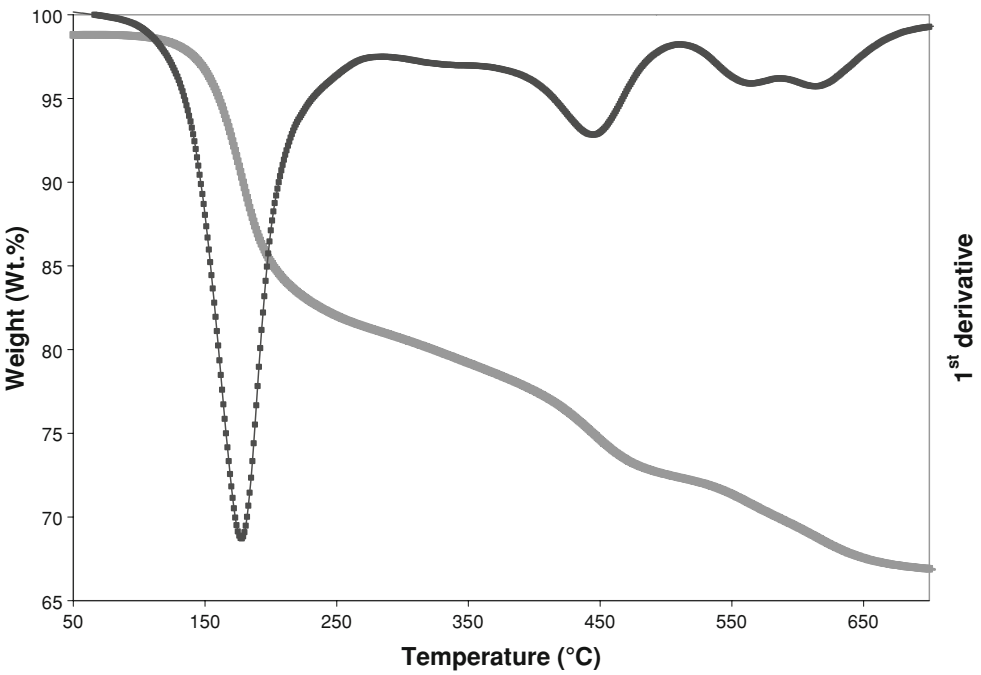

Fig. 5 Representative thermogravimetric weight loss under helium and derivative plot for PMO-$PFSO_3H$1.3

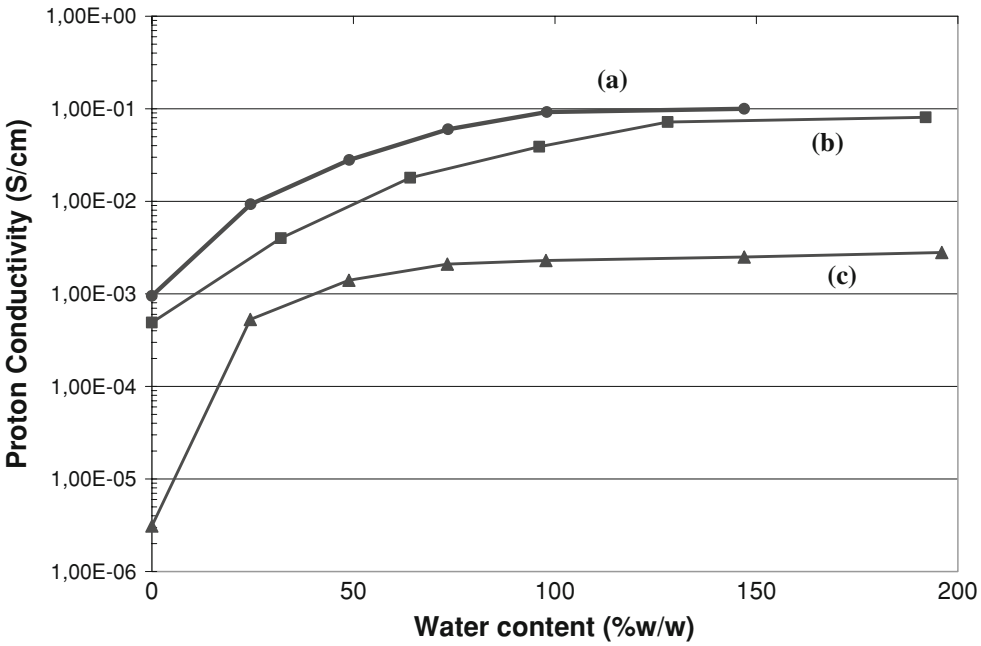

Fig. 7 RT proton conductivity as a function of water content for (*a*) PMO-PFSO$_3$H1.3, (*b*) PMO-PFSO$_3$H0.8, and (*c*) Nafion® SAC-13

Catalytic performance

The catalytic properties of the catalysts were evaluated in the self-condensation of heptanal at 30 and 75 °C (Fig. 9), which generates water. The analysis of the reaction products using GC-MS showed that the only product obtained was crotonaldehyde. This analysis showed no trace of the intermediate aldol product shown in Fig. 8a. Thus, the secondary dehydratation of the aldol product seems to be much faster than the primary aldol condensation. Figure 9 shows the heptanal conversion (calculated from the heptanal FTIR signals) over perfluoroalkylsulfonic acid-functionalized PMOs with a sulfur content of 0.83 and 1.27 mmol S/g for the same number of acid sites of PMO-PFSO$_3$H0.8 and PMO-FSO$_3$H1.3 in the reactor, respectively. Curves (a) and (b) being almost identical indicate that at the temperature of 75 °C, the density of acid sites does affect neither the specific catalytic activity nor the rate of deactivation since the same reaction rates are obtained when the comparison is made on the basis of the same number of acid sites. Curves (c) and (d) being also almost identical show that the above conclusion is also valid at 30 °C. Curves (e) and (f) were observed at 75 °C when using two acid-functionalized PMOs previously reported in our laboratory. Curve (e) corresponds to a phenylsulfonic acid-functionalized ethylene-silica (PMO-PSA in Table 1), and curve (f) corresponds to an arene sulfonic ethane-silica (ASMES in Table 1). The comparison between, on one hand, curves (a) and (b) with, on the other hand, curves (e) and (f) shows the much higher specific activity of the perfluoroalkyl sulfonic acid groups in PMO-PFSO$_3$H catalysts. Even at 30 °C [curves (c) and (d)], these catalysts show a significantly higher catalytic activity

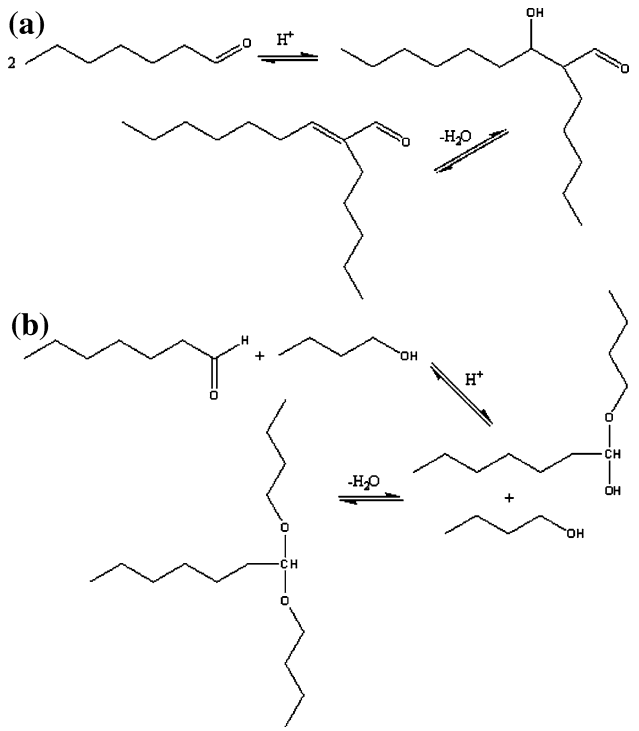

Fig. 8 Schematic representation of (**a**) self-condensation of heptanal and (**b**) acetalization of heptanal by 1-butanol over an acid catalyst

than the nonperfluoro-sulfonated sites at 75 °C. The conversion plateaus at 61 and 49% observed at 75 and 30 °C, respectively, suggest that the system reaches a chemical equilibrium under these conditions.

To illustrate the effect of the hybrid nature of the PMO walls on catalytic activity, a sample of perfluoroalkylsulfonic acid-grafted SBA-15 (pure silica of same pore structure)

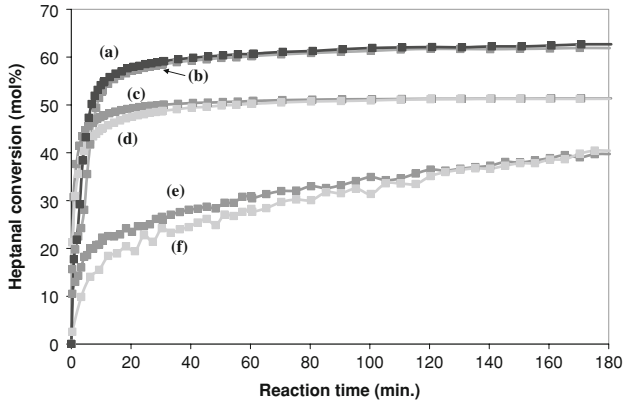

Fig. 9 Heptanal conversion for the self-condensation reaction over (*a*) 0.5 g of PMO-PFSO$_3$H0.8 at 75 °C, (*b*) 0.3 g of PMO-PFSO$_3$H1.3 at 75 °C, (*c*) 0.5 g of PMO-PFSO$_3$H0.8 at 30 °C, (*d*) 0.3 g of PMO-PFSO$_3$H1.3 at 30 °C, (*e*) 0.5 g of PMO-PSA at 75 °C, and (*f*) 0.5 g of ASMES at 75 °C (for the same number of acid sites in the reactor)

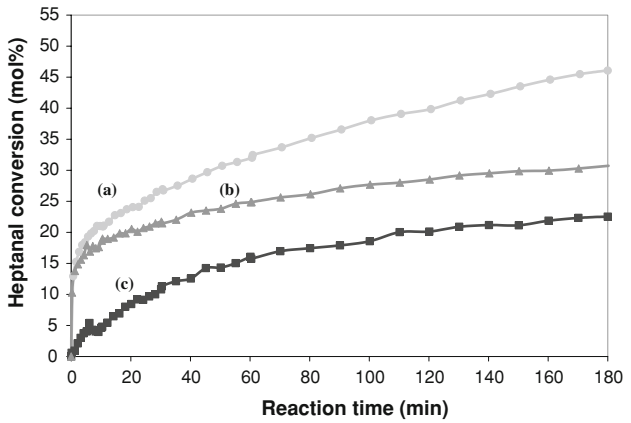

Fig. 10 Heptanal conversion for self-condensation reaction over (*a*) 0.046 g of PMO-PFSO$_3$H1.3, (*b*) 0.273 g of SBA-PFSO$_3$H0.2, and (*c*) 0.5 g Nafion SAC-13 at 75 °C (for the same number of acid sites in the reactor)

was prepared (see Table 1). Even though the preparation conditions of this sample were same as the ones of PMO-PFSO$_3$H0.8, the acid site density was much lower amounting to 0.25 mmol/g compared to 0.85 mmol/g. The comparison of catalytic performance is reported in Fig. 10. The same number of acid sites was introduced in the reactor for the catalysts PMO-PFSO$_3$H1.3, SBA-PFSO$_3$H0.2, and Nafion© SAC-13 which imposed a very small mass of the more acidic PMO-PFSO$_3$H1.3. It is seen from Fig. 10 that the specific activity of PMO-based catalyst is significantly higher than the SBA-15-based one.

Typical reusability tests performed with sample PMO-PFSO$_3$H1.3 are shown in Table 2. The sulfur content of the catalyst at the end of each of the 3-h tests is also reported in this table.

Table 2 Recycle studies of the PMOPFSO$_3$H1.3 catalyst at 75 °C

Reaction	Conversion (%)	Deactivation (%)	[S][a] (mmol/g) (±0.01)	Leaching (%)
1	62	–	0.94	28
2	45	27	0.81	38
3	41	35	0.73	43

[a] After reaction test

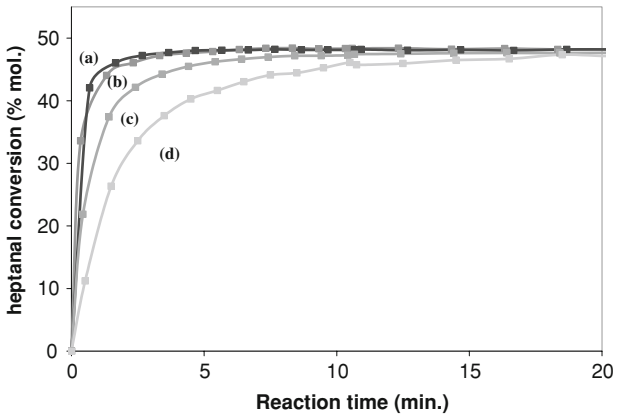

Fig. 11 Heptanal conversion for the acetalization of heptanal by 1-butanol at 75 °C for various catalysts (*a*) 0.05 g of PMO-PFSO$_3$H0.8, (*b*) 0.03 g of PMO-PFSO$_3$H1.3, (*c*) 0.048 g of PMO-PSA, and (*d*) 0.05 g of ASMES (for the same number of acid sites in the reactor)

The scheme of acetalization of heptanal by 1-butanol over an acid catalyst is presented in Fig. 8b. The heptanal conversion curves as functions of reaction time for different catalysts (for the same number of acid sites) are shown in Fig. 11. In this case, it is also possible to provide a direct comparison of specific activities per acid site for a reaction monitored at 75 °C. The conversion plateau is obtained at a heptanal conversion of 47% for all catalysts which also suggests a limitation by thermodynamic equilibrium [30]. The two PMO-PFSO$_3$H catalysts (plateau reached after 3 min) clearly exhibit a higher activity compared to PMO-PSA (10 min) and ASMES (15 min).

Discussion

The results presented above suggest that the chemical modification (grafting step) of the surface does not affect the structure of the support. There is no significant change in the XRD pattern recorded after the grafting step of THTSAS on PMO ethane-silica. In addition, only a diminution of specific surface area was observed as a result of the chemical modification of the PMO surface. Moreover, the hydrophobicity of the ethane-bridged PMO (even at high acid content, up to 1.30 mmol/g) allows a better diffusion of the β-sultone (THTSAS) in the PMO pore lattice

than in a mesostructured silica support (a 0.25 mmol/g of THTSAS was indeed grafted on both the calcined and ethanol-extracted SBA-15) which results in a higher density of grafted acid functions.

The acid properties (pyridine-FTIR, ion exchange capacity, CNS analysis, and proton conductivity) obtained for the perfluoroalkylsulfonic acid-functionalized PMOs are coherent with the literature for similar compounds [15, 23, 24, 33]. The FTIR spectra of chemisorbed pyridine showed the presence of only Brönsted acid sites for perfluoroalkylsulfonic acid-functionalized PMO catalysts. The predominance of Brönsted acid sites is confirmed by ion exchange capacity measurements since Lewis acid sites would not exchange ions from NaOH solutions.

The sulfonic acid-functionalized PMOs exhibited thermal stability up to 120 °C, which corresponds to the temperature of the beginning of the sulfonic acid function decomposition. The electronegative F atom tends to enhance the electron density in the C–F bond, thus weakening the Si–O–C bridge of the perfluoroalkylsulfonic acid functional group.

The higher activity per unit mass of PMO-$PFSO_3H$1.3 compared to PMO-$PFSO_3H$0.8 for both reactions is obviously ascribed to its higher density of acid sites (Table 1). The higher heptanal conversion for the self-condensation and acetalization obtained with PMO$PFSO_3H$1.3 materials in comparison with ASMES and PMO-PSA samples can be related to their stronger sulfonic acid sites. In this case, the perfluoroalkyl chain is more electrophilic than the benzene ring of the PMO-PSA hybrid sulfonic acid catalyst. The electrophilic effect of the perfluoroalkyl chain is so strong that the conversion of heptanal is higher at 30 °C for PMO-$PFSO_3H$1.3 than for both PMO-PSA and ASMES catalysts used at 75 °C for the self-condensation reaction. Furthermore, the highly hydrophobic character due to the presence of organic groups in the framework may allow a faster diffusion of heptanal toward the acid sites. The water produced can also be easily transferred out of the catalyst particle in the large hydrophobic mesopores and thus does not contribute as extensively to the acid site deactivation compared to silica-supported catalysts.

The reusability tests shown in Table 2 indicate that both sulfur lixiviation and loss activity of the materials acid sites contribute to deactivation. These results also suggest that sulfur-containing species in solution are not catalytically active.

Conclusion

The synthesis of perfluoroalkylsulfonic acid functionalized PMOs by a one-step chemical modification of an ethane-bridged PMO was described. This ethane-bridged PMO was synthesized using BTME as framework precursor under acidic conditions using Pluronic 123 as structure-directing agent. Surface OHs were then functionalized by grafting THTSAS. The resulting solid acid catalysts show high acid site density (up to 1.30 mmol H^+/g) and exceptional RT proton conductivity (up to 1.0×10^{-1} S/cm). These new perfluoroalkylsulfonic acid-functionalized PMOs exhibit a high catalytic activity in self-condensation of heptanal and heptanal acetalization by 1-butanol, owing to their high density of acid sites, their high acid site strength, and the presence of hydrophobic ethane-bridged framework. Indeed, the specific catalytic activity of the perfluoroalkylsulfonic acid sites in hydrophobic environments in materials such as PMO-$PFSO_3H$1.3 and PMO-$PFSO_3H$0.8 were shown to be higher than those of phenyl acid sites samples such as the ones of PMO-PSA and ASMES. This underlines the potential assets of PMOs and high-strength acid functions as catalysts supports in water-generating reactions whenever the acid sites are deactivated by water.

Acknowledgements The authors thank NSERC for financial support. The authors are grateful to G. Lemay, Dr. S. Mikhailenko, Dr. B. Nohair, and B. Levasseur for assistance in the experimental work.

References

1. Inagaki S, Guan S, Fukushima Y, Ohsuna T, Terasaki O (1999) J Am Chem Soc 121:9611. doi:10.1021/ja9916658
2. Melde BJ, Holland BT, Blanford CF, Stein A (1999) Chem Mater 11:3302. doi:10.1021/cm9903935
3. Asefa T, MacLachlan MJ, Coombs N, Ozin GA (1999) Nature 402:867
4. Inagaki S, Guan S, Ohsua T, Terasaki O (2002) Nature 416:304
5. Burleigh MC, Markowitz MA, Jayasundera S, Spector MS, Thomas CW, Gaber BP (2003) J Phys Chem B 107:12628. doi:10.1021/jp0351189q
6. Dag O, Yoshina-Ishii C, Asefa T, MacLachlan MJ, Grondey H, Coombs N, Ozin GA (2001) Adv Funct Mater 11:213
7. Goto Y, Inagaki S (2002) Chem Commun 2410
8. Hamoudi S, Kaliaguine S (2002) Chem Commun 2118
9. Kapoor MP, Yang Q, Inagaki S (2002) J Am Chem Soc 124:15176. doi:10.1021/ja0290678
10. Landskron K, Ozin GA (2005) Angew Chem Int Ed 44:2107. doi:10.1002/anie.2004462279
11. Garcia-Bennett AE, Yokoi T, Sakamoto K, Kunieda H, Terasaki O, Che S, Tatsumi T (2003) Nat Mater 2:801
12. Diaz I, Marquez-Alvarez C, Mohino F, Perez-Pariente J, Sastre E (2000) J Catal 193:283. doi:10.1006/jcat.20002898
13. Shimizu K, Hyaashi E, Hatmachi T, Kodama T, Higuchi T, Satsuma A, Kitayama Y (2005) J Catal 231:131. doi:10.1016/j.jcat.2005.01.017
14. Radu DR, Lai C-Y, Huang J, Shu X, Lin VS-L (2005) Chem Commun 1264
15. Alvaro M, Corma A, Das D, Fornés V, Garcia H (2004) Chem Commun 956
16. Alvaro M, Corma A, Das D, Fornés V, Garcia H (2005) J Catal 231:48. doi:10.1016/j.jcat.2005.01.007
17. Athens GL, Ein-Eli Y, Chmelka BF (2007) Adv Mater 19:2580. doi:10.1002/adma.200602781

18. Macquarrie DJ, Tavener SJ, Harmer MA (2005) Chem Commun 2363
19. Sow B, Hamoudi S, Zahedi-Niaki MH, Kaliaguine S (2005) Micropor Mesopor Mater 79:129. doi:10.1016/j.micromeso.2004.10.038
20. Margolese D, Melero JA, Christiansen SC, Chmelka BF, Stucky GD (2000) Chem Mater 12:2448. doi:10.1021/cm0010304
21. Yang Q, Kapoor MP, Inagaki S (2002) J Am Chem Soc 124:9694. doi:10.1021/ja026799r
22. Yang Q, Liu J, Yang J, Kapoor MP, Inagaki S, Li C (2004) J Catal 228:265. doi:10.1016/j.j.cat.2004.09.07
23. Yuan X, Lee HI, Kim JW, Yie JE, Kim JM (2003) Chem Lett 32:650. doi:10.1246/cl.2003.650
24. Yang Q, Kapoor MP, Inagaki S, Shirokura N, Kondo JN, Domen K (2005) J Mol Catal A 230:85. doi:10.1016/j.molcata.2004.12.010
25. Nakajima K, Tomita I, Hara M, Hayashi S, Domen K, Kondo JN (2005) Adv Mater 17:1839. doi:10.1002/adma.200500426
26. Nakajima K, Tomita I, Hara M, Hayashi S, Domen K, Kondo JN (2006) Catal Today 116:151. doi:10.1016/j.cattod.2006.01.022
27. Dubé D, Rat M, Béland F, Kaliaguine S (2008) Micropor Mesopor Mater 111:596. doi:10.1016/j.micromeso.2007.09.005
28. Melero JA, van Grieken R, Morales G, Paniagua M (2007) Energy Fuels 21:1782. doi:10.1021/ef060647
29. Lim MH, Blanford CF, Stein A (1998) Chem Mater 10:467
30. Rat M, Zahedi-Niaki MH, Kaliaguine S, Do T-O (2008) Micropor Mesopor Mater 112:26. doi:10.1016/j.micromeso.2007.09.010
31. Tsuji H, Yagi F, Hattori H, Kita H (1994) J Catal 148:759
32. Schimizu K, Hayashi E, Inokuchi T, Kodama T, Hagiwara H, Kitayama Y (2002) Tetrahedron Lett 43:9073
33. Climent MJ, Corma A, Iborra S, Navarro MC, Primo J (1996) J Catal 161:783
34. Tanaka Y, Sawamura N, Iwamoto M (1998) Tetrahedron Lett 39:9457
35. Choi M, Heo W, Kleitz F, Ryoo R (2003) Chem Commun 1340
36. Mikhailenko SD, Zaidi J, Kaliaguine S (1998) J Chem Soc Faraday Trans 94:1613
37. Hamoudi S, Royer S, Kaliaguine S (2004) Micropor Mesopor Mater 71:17. doi:10.1016/j.micromeso.2004.03.009
38. Ghanbari-Siahkali A, Philippou A, Garforth A, Cundy CS, Anderson MW, Dwyer J (2001) J Chem Mater 11:569